

## Supplementary Information

### **Structural Plasticity of SARS-CoV-2 3CL M<sup>pro</sup> Active Site Cavity Revealed by Room Temperature X-ray Crystallography**

Daniel W. Kneller,<sup>1</sup> Gwyndalyn Phillips,<sup>1</sup> Hugh M. O'Neill,<sup>1</sup> Robert Jedrzejczak,<sup>2,3</sup> Lucy Stols,<sup>2</sup> Paul Langan,<sup>1</sup> Andrzej Joachimiak,<sup>2,3,4</sup> Leighton Coates,<sup>1\*</sup> and Andrey Kovalevsky,<sup>1\*</sup>

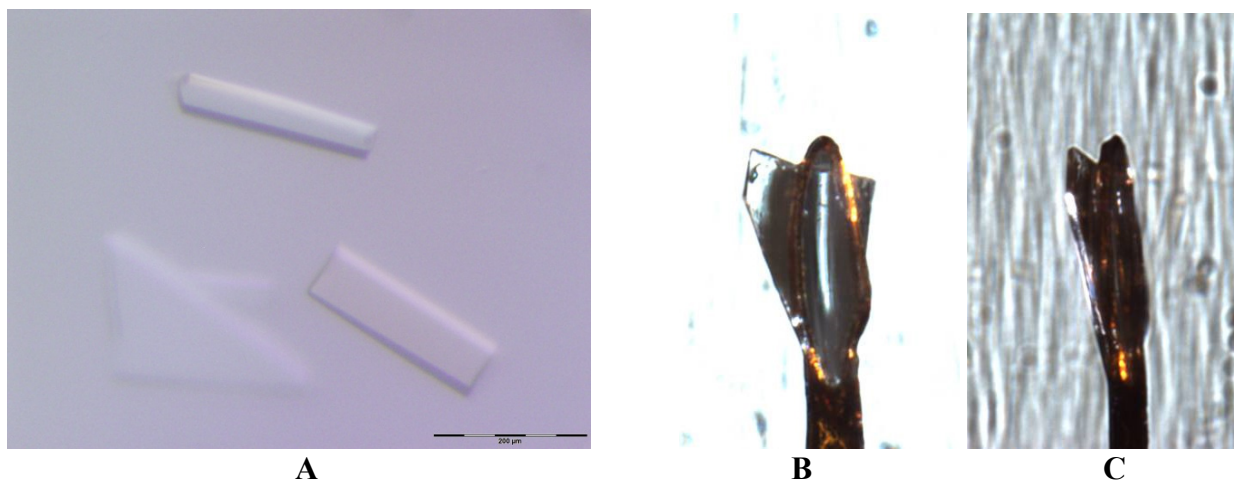
**Supplementary Table 1.** DNA sequence for the codon-optimized gene of SARS-CoV-2 3CL M<sup>pro</sup>.

AGCGCTGTTCTGCAGTCTGGTTTCCGTAAAATGGCTTTCCCGTCTGGTAAAGTTGAA  
GGTTGTATGGTTCAGGTAACCTGCGGCACTACCACCCTGAACGGCCTGTGGCTGGAT  
GACGTTGTTTACTGCCC GCGTCATGTTATCTGTACTTCCGAAGATATGCTGAACCCG  
AACTACGAAGATCTGCTGATCCGTAAATCTAACCACA ACTTCCCTGGTTCAGGCAGGT  
AACGTT CAGCTGCGTGTTATCGGTC ACTCTATGCAGAACTGCGTTCGAAACTGAAA  
GTTGATACCGCTAACCCGAAAACCCCGAAATACAAATTCGTTTCGTATCCAGCCGGGT  
CAGACCTTCAGCGTTCGGCTTGCTATAACGGTTCCTCCGTCTGGTGTTCACAGTGCG  
CTATGCGTCCGAACTTCACTATTAAAGGTTCCCTCCTGAACGGTTCCTGTGGTTCGT  
TGGTTTCAACATTGATTACGATTGCGTTTCTTTCTGCTACATGCACCACATGGA ACTG  
CCGACTGGTGTTCACGCTGGCACCGATCTGGAAGGTA ACTTTTACGGTCCGTTTCGTT  
GACCGTCAGACCGCTCAGGCTGCTGGTACTGATACCACCATACCGTTAACGTTCTG  
GCTTGGCTGTACGCTGCTGTTATCAACGGTGATCGTTGGTTCCTGAACCGTTTCACCA  
CCACCCTGAACGATTTCAACCTGGTTGCGATGAAATACA ACTACGAACCGCTGACCC  
AGGATCACGTTGACATCCTGGGTCCGCTGTCTGCTCAGACCGGTATCGCTGTTCTGG  
ATATGTGCGCTTCTCTGAAAGAACTGCTGCAGAACGGTATGAACGGTCGTACCATCC  
TGGGTTCTGCTCTGCTGGAAGATGAATTTACCCCGTTCGATGTTGTTTCGTCAGTGCTC  
TGGTGTTACCTTCCAGGGTCCGCATCATCACCATCACCAT

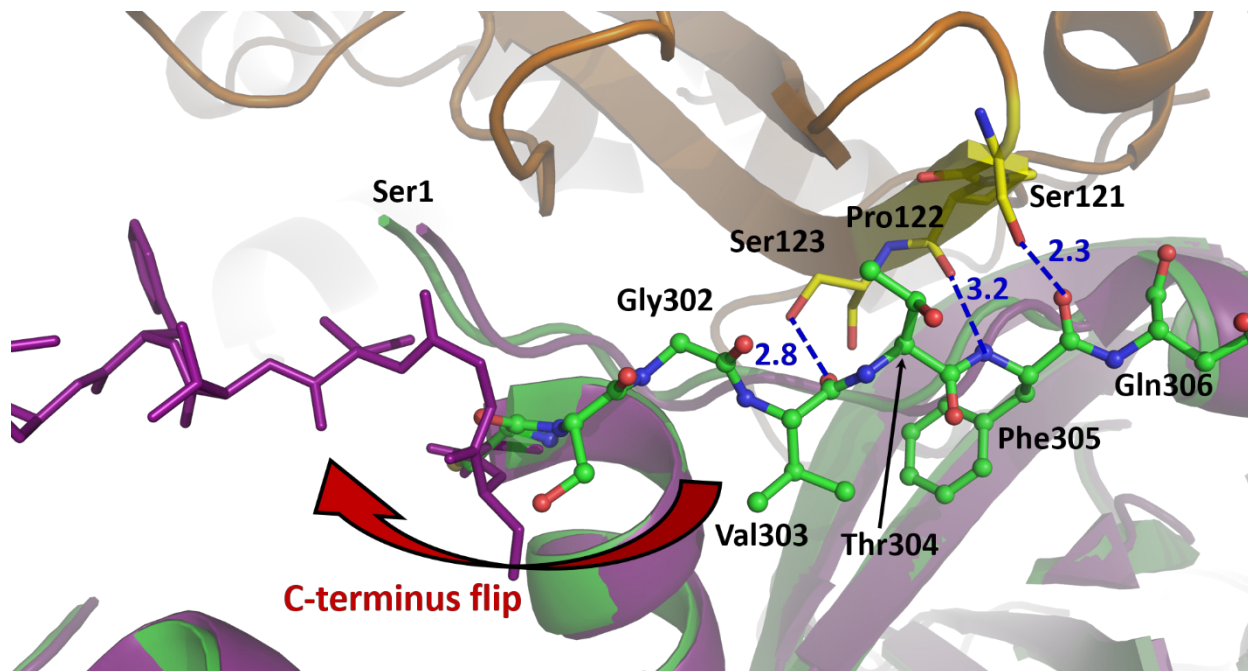
**Supplementary Table 2.** Data reduction and refinement statistics for the room temperature structure of the 3CL M<sup>pro</sup> from SARS-CoV-2.

<b>3CL M<sup>pro</sup>, PDB ID</b>	
<b>6WQF</b>	
<b>Data collection:</b>	<b>X-ray</b>
Diffractionmeter	Rigaku HighFlux Eiger 4M
Space group	I2
Wavelength (Å)	1.54
Cell dimensions:	
<i>a</i> , <i>b</i> , <i>c</i> (Å)	45.07, 54.06, 113.61
$\alpha$ , $\beta$ , $\gamma$ (°)	90, 100.51, 90
Resolution (Å)	27.92-2.30 (2.38-2.30)*
No. reflections unique	11514 (858)
<i>R</i> <sub>merge</sub>	0.110 (0.621)
<i>R</i> <sub>pim</sub>	0.065 (0.421)
<i>CC</i> <sub>1/2</sub>	0.993 (0.666)
<i>I</i> / $\sigma$ <i>I</i>	8.1 (1.9)
Completeness (%)	95.4 (72.6)
Redundancy	3.7 (2.7)
<b>Refinement:</b>	<b>X-ray</b>
Resolution	27.92 – 2.30
<i>R</i> <sub>work</sub> / <i>R</i> <sub>free</sub>	0.180 / 0.230
Ramachandran statistics	
Favored (%)	95.72
Allowed (%)	4.28
Outliers (%)	0
R.M.S. deviations	
Bond lengths (Å)	0.002
Bond angles (°)	0.444
All atom clashscore	0.85
<i>B</i> -factors (Å <sup>2</sup> )	
Protein (overall)	37.1
Protein (main chain)	35.4
Protein (side chain)	38.9
Water	32.6

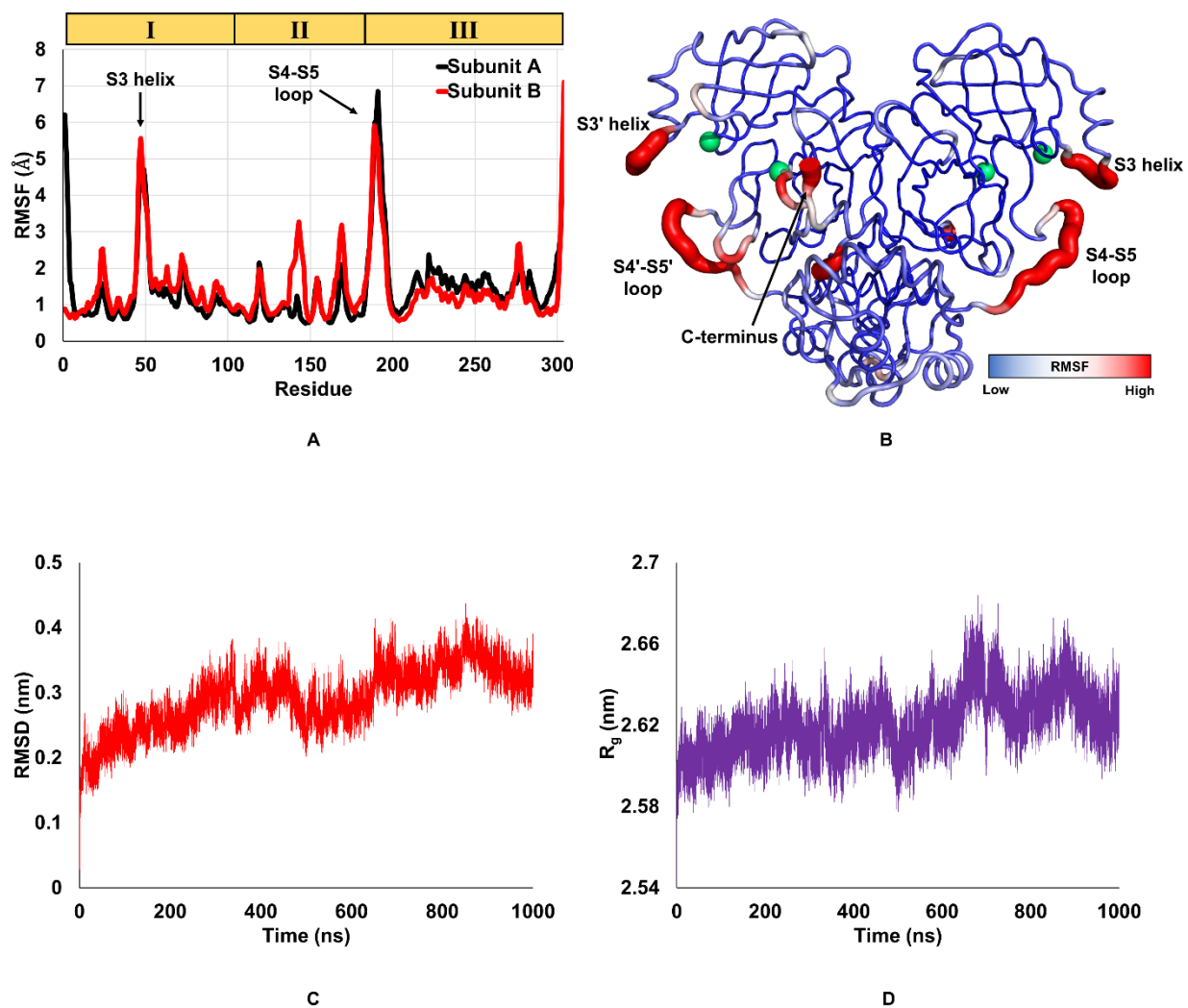
\* Values in parentheses are for highest-resolution shell. Data were collected from one crystal.



**Supplementary Figure 1.** (A) Crystals of 3CL M<sup>pro</sup> grown using the microseeding technique; (B, C) Crystal mounted on a loop used for the room-temperature X-ray data collection.



**Supplementary Figure 2.** Superposition of the room temperature ligand-free structure of 3CL M<sup>Pro</sup> (green carbon atoms) in complex with inhibitor N3 (deep purple, PDB ID 6LU7) from SARS-CoV-2. The C-terminal tail flips 180° upon the inhibitor binding (shown by the curved red arrow).



**Supplementary Figure 3.** Root Mean Square Fluctuation (RMSF) analysis from a 1 μs MD simulation of an apo 3CL M<sup>pro</sup> dimer. **(A)** Protein backbone RMSF by residue for Subunits A and B. **(B)** Cartoon-putty representation of 3CL M<sup>pro</sup> colored by protein backbone RMSF with Cα of His41/41' and Cys145/145' shown as green spheres. **(C)** RMSD of backbone atoms relative to the equilibrated structure. **(D)** Radius of gyration ( $R_g = 26.2 \pm 0.15 \text{ \AA}$ ) of 3CL M<sup>pro</sup> dimer.